Chapter 4

Stopping Power of Ions in a Magnetized Plasma: Binary Collision Formulation

Hrachya B. Nersisyan, Günter Zwicknagel and Claude Deutsch

Additional information is available at the end of the chapter

http://dx.doi.org/10.5772/intechopen.77213

Abstract

In this chapter, we investigate the stopping power of an ion in a magnetized electron plasma in a model of binary collisions (BCs) between ions and magnetized electrons, in which the two-body interaction is treated up to the second order as a perturbation to the helical motion of the electrons. This improved BC theory is uniformly valid for any strength of the magnetic field and is derived for two-body forces which are treated in Fourier space without specifying the interaction potential. The stopping power is explicitly calculated for a regularized and screened potential which is both of finite range and less singular than the Coulomb interaction at the origin. Closed expressions for the stopping power are derived for monoenergetic electrons, which are then folded with an isotropic Maxwell velocity distribution of the electrons. The accuracy and validity of the present model have been studied by comparisons with the classical trajectory Monte Carlo numerical simulations.

Keywords: ion stopping, magnetized plasma target, binary collisions

1. Introduction

There is an ongoing in the theory of interaction of charged particle beams with plasmas. Although most theoretical works have reported on the energy loss of ions in a plasma without magnetic field, the strongly magnetized case has not yet received as much attention as the field-free case. The energy loss of ion beams and the related processes in magnetized plasmas are important in many areas of physics such as transport, heating, magnetic confinement of thermonuclear plasmas, and astrophysics. The range of the related topics includes ultracold plasmas [1, 2], the

cooling of heavy ion beams by electrons [3–12], as well as many very dense systems involved in magnetized target fusions [11], or heavy ion inertial confinement fusion (ICF).

For a theoretical description of the energy loss of ions in a plasma, there exist some standard approaches. The dielectric linear response (LR) treatment considers the ion as a perturbation of the target plasma, and the stopping is caused by the polarization of the surrounding medium. It is generally valid if the ion couples weakly to the target. Since the early 1960s, a number of calculations of the stopping power (SP) within LR treatment in a magnetized plasma have been presented (see Refs. [13–37] and references therein). Alternatively, the stopping is calculated as a result of the energy transfers in successive binary collisions (BCs) between the ion and the electrons [37–45]. Here, it is necessary to consider appropriate approximations for the screening of the Coulomb potential by the plasma [8]. However, significant gaps between these approaches involve the ion stopping along magnetic field **B** and perpendicular to it. In particular, at high B values, the BC predicts a vanishingly parallel energy loss, which remains at variance with the nonzero LR one. Also, challenging BCLR discrepancies persist in the transverse direction, especially for vanishingly small ion projectile velocity v_i when the friction coefficient contains an anomalous term diverging logarithmically at $\mathbf{v_i} = 0$ [23, 24]. For calculation of the energy loss of an ion, two new alternative approaches have been recently suggested. One of these methods is specifically aimed at a low-velocity energy loss, which is expressed in terms of velocity-velocity correlation and, hence, to a diffusion coefficient [34]. Next, in Ref. [27] using the Bhatnagar-Gross-Krook approach based on the Boltzmann-Poisson equations for a collisional and magnetized classical plasma, the energy loss of an ion is studied through a LR approach, which is constructed such that it conserves particle number locally.

An alternative approach, particularly in the absence of any relevant experimental data, is to test various theoretical methods against comprehensive numerical simulations. This can be achieved by a particle-in-cell (PIC) simulation of the underlying nonlinear Vlasov-Poisson Equation [10, 31]. While the LR requires cutoffs to exclude hard collisions of close particles, the collectivity of the excitation can be taken into account in both LR and PIC approaches. In the complementary BC treatment, the stopping force has been calculated numerically by scattering statistical ensembles of magnetized electrons from the ions in the classical trajectory Monte Carlo (CTMC) method [7, 10, 37–41]. For a review we refer to a recent monograph [8] which summarizes all theoretical and numerical methods and approaches also discussing the ranges of their validity.

The very recent upheaval of successful experiments involving hot and dense plasmas in the presence of kilotesla magnetic fields (e.g., at ILE (Osaka), CELIA (Bordeaux), LULI (Palaiseau), LLNL (Livermore)) remaining nearly steady during 10–15 ns strongly motivates the fusion as well as the warm dense matter (WDM) communities to investigate adequate diagnostics for their dynamic properties. This opens indeed a novel perspective by allowing magnetic fields to play a much larger if not a central role both in ICF and WDM plasmas. In this context proton or any nonrelativistic ion stopping is likely to provide an option of choice for investigating genuine magnetization features such as anisotropy, when the electron plasma frequency turns significantly lower than the cyclotron one [46]. In addition, an experimental test of proton or alpha particle stopping in a magnetized plasma is currently envisioned (see, e.g., Ref. [46] for a preliminary discussion). The parameters at hand are a fully ionized hydrogen plasma with a density up to $10^{20}\,\mathrm{cm}^3$ and temperature between 1 and 100 eV. The steady magnetic field can be up to 45 T strong. A preliminary examination based on comparing electron Debye length

with corresponding Larmor radius indicates that to experience a strong influence of the magnetic field, the electron density should be comparable with a few 10^{16} cm^3. We expect these endeavors to lead to the very first unambiguous and genuine identification of an experimental magnetic signature for nonrelativistic ion stopping in plasmas.

Motivated by these recent developments, our purpose is to investigate the SP of an ion moving in a magnetized plasma in a wide range of the value of a steady magnetic field. The present paper is based on our earlier studies in Refs. [8, 24, 44, 45] where the second-order energy transfers for individual collisions of electron-ion [8, 24, 44] of any two identical particles, like electron-electron [44], and finally of two gyrating arbitrary charged particles [45] have been calculated with the help of an improved BC treatment. This treatment is—unlike earlier approaches of, e.g., Refs. [9, 42]—valid for any strength of the magnetic field. As the first application of the theoretical BC model developed in Refs. [8, 24, 44, 45], we have calculated in Ref. [47] the cooling forces on the heavy ion beam interacting with a strongly magnetized and temperature anisotropic electron beam. It has been shown that there is a quite good overall agreement with both the CTMC numerical simulations and the experiments performed at the ESR storage ring at GSI [48–50].

In Section 2 we introduce briefly a perturbative binary collision formulation in terms of the binary force acting between an ion and a magnetized electron and derive general expressions for the second-order (with respect to the interaction potential) stopping power. In contrast to the previous investigations in Refs. [8, 24, 44, 45], we here consider the (macroscopic) stopping force which is obtained by integrating the binary force of an individual electron-ion interaction with respect to the impact parameter and the velocity distribution function of electrons. That is, the stopping force for monoenergetic electrons is folded with a velocity distribution. The resulting expressions involve all cyclotron harmonics of the electrons' helical motion and are valid for any interaction potential and any strength of the magnetic field. In Section 2.4 we present explicit analytic expressions of this second-order stopping power for the specific case of a regularized and screened interaction potential [51, 52] which is both of finite range and less singular than the Coulomb interaction at the origin and which includes as limiting cases the Debye (i.e., screened) and the Coulomb potentials. For comparison of our expressions with previous approaches, we consider in Section 3 the corresponding asymptotic expressions for large and small ion velocities and strong and vanishing magnetic fields. The analytical expressions presented in Section 2.4 are evaluated numerically in Section 4 using parameters of the envisaged experiments on ion stopping [46]. In particular, we compare our approach with the CTMC simulations. The results are summarized and discussed in Section 5. The regularization parameter and the screening length involved in the interaction potential are briefly specified and discussed in Appendix A.

2. Theoretical model

2.1. Binary collision (BC) formulation

Let us consider two point charges with masses m, M and charges $-e, Ze$, respectively, moving in a homogeneous magnetic field $\mathbf{B} = B\mathbf{b}$. We assume that the particles interact with the potential $-Z\not{e}^2U(r)$ with $\not{e}^2 = e^2/4\pi\epsilon_0$, where ϵ_0 is the permittivity of the vacuum and

$\mathbf{r} = \mathbf{r}_1 - \mathbf{r}_2$ is the relative coordinate of the colliding particles. For two isolated charged particles, this interaction is given by the Coulomb potential, i.e., $U_C(\mathbf{r}) = 1/r$. In plasma applications U_C is modified by many-body effects and the related screening and turns into an effective interaction. In general, this effective interaction, which is related to the wake field induced by a moving ion, is non-spherically symmetric and depends also on the ion velocity. For any BC treatment, however, this complicated ion-plasma interaction must be approximated by an effective two-particle interaction $U(\mathbf{r})$. This effective interaction U may be modeled by a spherically symmetric Debye-like screened interaction $u_D(\mathbf{r}) = e^{-r/\lambda}/r$ with a screening length λ, given, e.g., by the Debye screening length λ_D (see, e.g., [16]), in case of low ion velocities and an effective velocity-dependent screening length $\lambda(v_i)$ for larger ion velocities v_i (see [53–55]). Further details on the choice of the effective interaction $U(r)$ are given in Ref. [47].

In the presence of an external magnetic field, the Lagrangian and the corresponding equations of particle motion cannot, in general, be separated into parts describing the relative motion and the motion of the center of mass (cm) [8]. However, in the case of heavy ions, i.e., $M \gg m$, the equations of motion can be simplified by treating the cm velocity $\mathbf{v}_{\mathrm{cm}}$ as constant and equal to the ion velocity $\mathbf{v}_i$, i.e., $\mathbf{v}_{\mathrm{cm}} = \mathbf{v}_i = const$. Then, introducing the velocity correction through relations $\delta v_{(t)} = \mathbf{v}_e(t) - \mathbf{v}_{e0}(t) = \mathbf{v}(t) - \mathbf{v}_0(t)$, where $\mathbf{v}(t) = r(t) = \mathbf{v}_e(t) - \mathbf{v}_i$ is the relative electron-ion velocity $\mathbf{v}_{e0}(t)$ and $\mathbf{v}_0(t) = \dot{\mathbf{r}}_0(t) = \mathbf{v}_{e0}(t) - \mathbf{v}_i$ are the unperturbed electron and relative velocities, respectively, the equation of relative motion turns into

$$r_0(t) = \mathbf{R}_0 + \mathbf{v}_r t + a[\mathbf{u}\sin(\omega_c t) - [\mathbf{b} \times \mathbf{u}]\cos(\omega_c t)], \tag{1}$$

$$\delta\dot{\mathbf{v}}(t) + \omega_c[\delta\mathbf{v}(t) \times \mathbf{b}] = -\frac{Z\ell^2}{m}\mathbf{f}[\mathbf{r}(t)]. \tag{2}$$

Here, $-Z\ell^2\mathbf{f}[\mathbf{r}(t)](\mathbf{f} = -\partial U/\partial\mathbf{r})$ is the force exerted by the ion on the electron, $\omega_c = eB/m$ is the electron cyclotron frequency, and $\delta\mathbf{v}(t) \to 0$ at $t \to -\infty$. In Eq. (1) $\mathbf{u} = (\cos\varphi, \sin\varphi)$ is the unit vector perpendicular to the magnetic field; the angle φ is the initial phase of the electron's helical motion; $\mathbf{v}_r = v_{e\|}\mathbf{b} - \mathbf{v}_i$ is the relative velocity of the guiding center of the electrons, where $v_{e\|}$ and $v_{e\perp}$ (with $v_{e\perp} \leq 0$) are the unperturbed components of the electron velocity parallel and perpendicular to $\mathbf{b}$, respectively; and $a = v_{e\perp}/\omega_c$ is the cyclotron radius. In Eq. (1), the quantities $\mathbf{u}$ and $\mathbf{R}_0$ are defined by the initial conditions. In Eq. (2) $\mathbf{r}(t) = \mathbf{r}_e(t) - \mathbf{v}_i t$ is the ion-electron relative coordinate.

2.2. The perturbative treatment

We seek an approximate solution of Eq. (2) in which the interaction force between the ion and electron is considered as a perturbation. Thus, we are looking for a solution of Eq. (2) for the variables $\mathbf{r}$ and $\mathbf{v}$ in a perturbative manner $\mathbf{r} = \mathbf{r}_0 + \mathbf{r}_1 + \ldots, \mathbf{v} = \mathbf{v}_0 + \mathbf{v}_1 + \cdots$, where $\mathbf{r}_0(t), \mathbf{v}_0(t)$ are the unperturbed ion-electron relative coordinate and velocity, respectively, and $\mathbf{r}_n(t), \mathbf{v}_n(t)(n = 1, 2, \cdots)$ are the nth-order perturbations of $\mathbf{r}(t)$ and $\mathbf{v}(t)$, which are proportional to Z^n.

The parameter of smallness which justifies such kind of expansion can be read off from a dimensionless form of the equation of motion Eq. (2) by scaling lengths in units of the screening length λ, velocities in units of the initial relative velocity v_0, and time in units of λ/v_0. Then, it is seen (see Ref. [47] for details) that the perturbative treatment is essentially applicable in cases where $|Z|\phi^2/mv_0^2\lambda < 1$, that is, when the (initial) kinetic energy of relative motion $mv_0^2/2$, is large compared to the characteristic potential energy $|Z|\phi^2/\lambda$ in a screened Coulomb potential. Or, expressed in velocities, the initial relative velocity v0 must exceed the characteristic velocity $v_d = \left(|Z|\phi^2/m\lambda\right)^{1/2}$, that is, v_d here demarcates the perturbative from the nonperturbative regime. If this condition is met not only for a single ion-electron collision but in the average over the electron distribution, e.g., by replacing v0 with the averaged initial ion-electron relative velocity $\langle v_0\rangle$, i.e., $\langle v_0\rangle \gtrsim v_d$, we are in a regime of weak ion-target or, here, weak ion-electron coupling, which allows the use of perturbative treatments (besides BC also, e.g., linear response (LR)). For nonmagnetized electrons this is discussed in much detail in Refs. [53, 54]. Even though the particle trajectories are much more intricate in the presence of an external magnetic field, the given definitions and demarcations of coupling regimes are basically the same for magnetized electrons. That is, the applicability of a perturbative treatment is essentially related to the charge state Z of the ion and the typical range λ of the effective interaction, but not directly on the strength B of the magnetic field. The latter may affect the critical velocity v_d only implicitly via a possible change of the effective screening length λ with B.

The equation for the first-order velocity correction is obtained from Eq. (2) replacing on the right-hand side of the exact relative coordinate $\mathbf{r}(t)$ by $\mathbf{r}_0(t)$ with the solutions $\mathbf{v}_1(t) = \dot{\mathbf{r}}_1(t)$ and

$$r_1(t) = \frac{Z\phi^2}{m}\left\{-\mathbf{b}\mathcal{Q}_{\parallel}(t) + Re[\mathbf{b}(\mathbf{b}\cdot\mathcal{Q}_{\perp}(t)) - \mathcal{Q}_{\perp}(t) + i[\mathbf{b}\times\mathcal{Q}_{\perp}(t)]]\right\}. \tag{3}$$

Here, we have introduced the following abbreviations:

$$\begin{aligned}\mathcal{Q}_{\parallel}(t) &= \int_{-\infty}^{t} \mathbf{b}\cdot\mathbf{f}[\mathbf{r}_0(\tau)](t-\tau)d\tau,\\ \mathcal{Q}_{\perp}(t) &= \frac{1}{i\omega_c}\int_{-\infty}^{t}\mathbf{f}[\mathbf{r}_0(\tau)]\left[e^{\omega_c(t-\tau)}-1\right]d\tau\end{aligned} \tag{4}$$

and have assumed that all corrections vanish at $t \to -\infty$.

2.3. Second-order stopping power

We now consider the interaction process of an individual ion with a homogeneous electron plasma described by a velocity distribution function $f(\mathbf{v}_e)$ and a density n_e. We assume that the ion experiences independent binary collisions (BCs) with the electrons. The total stopping force, $\mathbf{F}(\mathbf{v}_i)$, acting on the ion is then obtained by multiplying the binary force $Z\phi^2\mathbf{f}[\mathbf{r}(t)]$ by the element of the flux relative flux $n_e v_r d^2 s dt$, integrating with respect to time and folding with velocity distribution of the electrons. The impact parameter s introduced here in the electron flux is defined by $s = \mathbf{R}_{0\perp} = \mathbf{R}_0 - \mathbf{n}_r(\mathbf{n}_r\cdot\mathbf{R}_0)$ and is the component of $\mathbf{R}_0$ perpendicular to the

relative velocity vector $\mathbf{v}_r$ with $\mathbf{n}_r = \mathbf{v}_r/v_r$. As can be inferred from Eq. (1), s represents the distance of the closest approach between the ion and the guiding center of the electron's helical motion.

The resulting stopping power, $S(\mathbf{v}_i) = -\frac{\mathbf{v}_i}{v_i} \cdot \mathbf{F}(\mathbf{v}_i)$, then reads

$$S(\mathbf{v}_i) = -\frac{Ze^2 n_e}{v_i} \int d\mathbf{v}_e f(\mathbf{v}_e) v_r \int d^2\mathrm{s} \int_{-\infty}^{\infty} \mathbf{v}_i \cdot \mathbf{f}[\mathbf{r}(t)] dt, \tag{5}$$

which is an exact relation for uncorrelated BCs of the ion with electrons. We evaluate this expression within a systematic perturbative treatment (see Ref. [47] for more details). First, we introduce the two-particle interaction potential $U(r)$, and the binary force $\mathbf{f}(\mathbf{r})$ is written using Fourier transformation in space. Furthermore, the factor $e^{i\mathbf{k}\cdot\mathbf{r}(t)}$ in the Fourier transformed binary force is expanded in a perturbative manner as $e^{i\mathbf{k}\cdot\mathbf{r}(t)} \simeq e^{i\mathbf{k}\cdot\mathbf{r}_0(t)}[1 + i(\mathbf{k}\cdot\mathbf{r}_1(t))]$, where $\mathbf{r}_0(t)$ and $\mathbf{r}_1(t)$ are the unperturbed and the first-order corrected relative coordinates (Eqs. (1) and (3)), respectively. Next, we consider only the second-order binary force $\mathbf{f}_2$ and the corresponding stopping force $\mathbf{F}_2$ with respect to the binary interaction since the averaged first-order force $\mathbf{F}_1$ (related to $\mathbf{f}_1$) vanishes due to symmetry reasons [8, 24, 44, 45, 47]. Within the second-order perturbative treatment, the stopping power can be represented as

$$S(\mathbf{v}_i) = -\frac{Z\not{e}^2 n_e}{v_i} \int d\mathbf{v}_e f(\mathbf{v}_e) v_r \int d^2\mathbf{s} \int d\mathbf{k} U(\mathbf{k}) (\mathbf{k}\cdot\mathbf{v}_i) \int_{-\infty}^{\infty} [\mathbf{k}\cdot\mathbf{r}_1(t)] e^{i\,\mathbf{k}\cdot\mathbf{r}_0(t)} dt. \tag{6}$$

From Eq. (6) it is seen that the second-order stopping power is proportional to Z^2. Inserting now Eqs. (1) and (3) into Eq. (6), assuming an axially symmetric velocity distribution $f(\mathbf{v}_e) = f(v_{e\|}, v_{e\perp})$, and performing the s integration, we then obtain

$$\begin{aligned} S = &-\frac{(2\pi)^4 Z^2 \not{e}^4 n_e}{m v_i} \int_{-\infty}^{\infty} dv_{e\|} \int_0^{\infty} f(v_{e\|}, v_{e\perp}) v_{e\perp} dv_{e\perp} \\ &\times \int d\mathbf{k} |U(\mathbf{k})|^2 (\mathbf{k}\cdot\mathbf{v}_i) \int_0^{\infty} \left[k_{\|}^2 + k_{\perp}^2 \frac{\sin(\omega_c t)}{\omega_c t} \right] \\ &\times J_0\left(2k_{\perp} a \sin\frac{\omega_c t}{2} \right) \sin(\mathbf{k}\cdot\mathbf{v}_r t) dt d, \end{aligned} \tag{7}$$

where J_n is the Bessel function of the nth order; $k_{\|} = (\mathbf{k}\cdot\mathbf{b})$ and $k_{\perp}$ are the components of $\mathbf{k}$ parallel and transverse to $\mathbf{b}$, respectively; and $v_{e\|}$ and $v_{e\perp}$ are the electron velocity components parallel and transverse to $\mathbf{b}$, respectively. This general expression (7) for the stopping power of an individual ion has been derived within second-order perturbation theory but without any restriction on the strength of the magnetic field B.

2.4. The SP for a regularized and screened coulomb potential

For an electron plasma with an isotropic Maxwell distribution, the velocity distribution relevant for the averaging in Eq. (7) is given by

$$f(v_e) = \frac{1}{(2\pi)^{3/2} v_{\text{th}}^3} e^{-v_e^2/2v_{\text{th}}^2}, \tag{8}$$

where the thermal velocity v_th is related to the electron temperature by $v_{\text{th}}^2 = T/m$ (here, the temperature is measured in energy units). Inserting Eq. (8) into expression (7) and assuming now a spherically symmetric potential $U = U(k)$ yields after performing the velocity integrations (see Ref. [56]), the stopping power

$$\begin{aligned} S(v_i) = \frac{8Z^2 \not{e}^4 n_e}{m\omega_c v_i} \frac{(2\pi)^4}{4} \int_0^\infty dk_\parallel \int_0^\infty U^2(k) k_\perp dk_\perp \int_0^\infty e^{-\frac{t^2}{2}k_\parallel^2 a^2} e^{-k_\perp^2 a^2 (1-\cos t)} \left(k_\parallel^2 + k_\perp^2 \frac{\sin t}{t} \right) t dt \\ \times \left[k_\perp a_{i\perp} \cos\left(k_\parallel a_{i\parallel} t\right) J_1(k_\perp a_{i\perp} t) + k_\parallel a_{i\parallel} \sin\left(k_\parallel a_{i\parallel} t\right) J_0(k_\perp a_{i\perp} t) \right]. \end{aligned} \tag{9}$$

Here, we have introduced the thermal cyclotron radius of the electrons $a = v_{th}/\omega_c$, and $a_{i\perp} = v_{i\perp}/\omega_c$, $a_{i\parallel} = v_{i\parallel}/\omega_c$, where $v_{i\perp}$ and $v_{i\parallel}$ are the ion velocity components transverse and parallel to b, respectively. For the Coulomb interaction $U(k) = U_C(k)$, the full two-dimensional integration over the s-space results in a logarithmic divergence of the k integration in Eqs. (7) and (9). To cure this, cutoff parameters $k_{\min}$ and $k_{\max}$ must be introduced (see, e.g., Refs. [8, 24, 47] for details). These cutoffs are related to the screening of the interaction in a plasma target and the incorrect treatment of hard collisions in a classical perturbative approach. As an alternative implementation of this standard cutoff procedure, we here employ the regularized screened interaction $U(r) = U_R(r) = \left(1 - e^{-r/\lambda}\right) e^{-r/\lambda}/r$ with the Fourier transform

$$U_R(k) = \frac{2}{(2\pi)^2} \left(\frac{1}{k^2 + \lambda^{-2}} - \frac{1}{k^2 + d^{-2}} \right), \tag{10}$$

where $d^{-1} = \lambda^{-1} + \text{ƛ}^{-1}$. U_R represents a Debye-like screened interaction U_D (see Section 2.1) which is additionally regularized at the origin [51, 52] and thus removes the problems related to the Coulomb singularity in a classical picture and prevents particles (for $Z > 0$) from falling into the center of the potential. The parameter λ related to this regularization is here considered as a given constant or as a function of the classical collision diameter [47].

Substituting the interaction potential (10) into Eq. (9) and performing the $k_\parallel$ integration, we arrive, after lengthy but straightforward calculations, at

$$\begin{aligned} S(v_i) = \frac{4\sqrt{\pi} Z^2 \not{e}^4 n_e}{m v_{\text{th}}^2} v \int_0^\infty \frac{dt}{t} \int_0^1 d\zeta \exp\left[-v^2 \zeta^2 P(t,\zeta) \right] \Phi[\Psi(t,\zeta)] \\ \times \left[P_1(t,\zeta) + \frac{\sin(\alpha t)}{\alpha t} P_2(t,\zeta) \right] \frac{\zeta^2 (1-\zeta^2)}{G(t,\zeta)}, \end{aligned} \tag{11}$$

where $P(t,\zeta) = \cos^2\vartheta + \sin^2\vartheta / G(t,\zeta)$ and

$$P_1(t,\zeta) = 2\cos^2\vartheta + P(t,\zeta)\left(1 - 2v^2\zeta^2\cos^2\vartheta\right), \tag{12}$$

$$P_2(t;\zeta) = \frac{2}{G(t,\zeta)} \left[\frac{\sin^2\vartheta}{G(t,\zeta)} + P(t,\zeta) \left(1 - \frac{v^2\zeta^2 \sin^2\vartheta}{G(t,\zeta)} \right) \right]. \tag{13}$$

Here, we have introduced the dimensionless quantities $v = v_i/\sqrt{2}v_{\mathrm{th}}$, $\alpha = \omega_c\lambda/v_{\mathrm{th}}$. ϑ is the angle between b and v_i, $\Psi(t,\zeta) = \left(t^2/2\right)\left(1-\zeta^2\right)/\zeta^2$, $G(t,\zeta) = \Theta(t)\zeta^2 + 1 - \zeta^2$, $\Theta(t) = \left(\frac{2}{\alpha t}\sin\frac{\alpha t}{2}\right)^2$, and

$$\Phi(z) = e^{-z} + e^{-\varkappa^2 z} - \frac{2}{\varkappa^2 - 1}\frac{1}{z}\left(e^{-z} - e^{-\varkappa^2 z}\right), \tag{14}$$

where $\varkappa = \lambda/d = 1 + \lambda/\lambda\!\!\!^{-}$.

Eq. (11) for the SP is the main result of the outlined BC treatment which will now be evaluated in the next sections.

3. Comparison with previous approaches

Previous theoretical expressions for the stopping power which have been extensively discussed by the plasma physics community (see, e.g., Refs. [3, 8] for reviews) basically concern the two limiting cases of vanishing and infinitely strong magnetic fields. We therefore investigate the present approach for these two cases, first for arbitrary interactions $U(\mathbf{k})$ and electron distributions $f(\mathbf{v}_e)$ as given by Eq. (7) and later for the more specific situation of the regularized interaction (10) and the velocity distribution (8) as given by Eq. (11).

3.1. General SP Eq. (7) at vanishing and infinitely strong magnetic fields

At vanishing magnetic field $(B \to 0)$, $\sin(\omega_c t)/(\omega_c t) \to 1$ and the argument of the Bessel function in Eq. (7) should be replaced by $k_\perp v_{e\perp} t$. Then, denoting the second-order SP at vanishing magnetic field as S_0 and assuming spherically symmetric potential with $U = U(k)$, one obtains

$$S_0(\mathbf{v}_i) = \frac{4(2\pi)^2 Z^2 e^4 n_e}{m v_i^2} \quad \mathcal{U}\int_0^{v_i} f(v_e) v_e^2 dv_e, \tag{15}$$

where $\mathcal{U}$ is the generalized Coulomb logarithm:

$$\mathcal{U} = \frac{(2\pi)^4}{4}\int_0^\infty U^2(k) k^3 dk. \tag{16}$$

Employing the regularized and screened potential $U(k)$ given by Eq. (10), the generalized Coulomb logarithm is $\mathcal{U} = \mathcal{U}_R = \Lambda(\varkappa)$ (see also Refs. [8, 24, 44, 45]), where

$$\Lambda(\varkappa) = \frac{\varkappa^2 + 1}{\varkappa^2 - 1}\ln\varkappa - 1. \tag{17}$$

Taking the bare Coulomb interaction with $U(k) = U_C(k) \sim 1/k^2$, Eq. (16) diverges logarithmically at $k \to 0$ and $k \to \infty$, and two cutoffs $k_{\min} = 1/r_{\max}$ and $k_{\max} = 1/r_{\min}$ must be introduced

as discussed in Section 2.4. In this case the generalized Coulomb logarithm takes the standard form $\mathcal{U} = \mathcal{U}_C = \ln(k_{\max}/k_{\min}) = \ln(r_{\max}/r_{\min})$.

The asymptotic expression of Eq. (15) at high ion velocities can be easily derived using the normalization of the distribution function which results in

$$S_0(\mathbf{v}_i) \simeq \frac{4\pi Z^2 \not{e}^4 n_e}{m v_i^2}\ \mathcal{U}. \tag{18}$$

At an infinitely strong magnetic field ($B \to \infty$), the term in Eq. (7) proportional to $k_\perp^2$ and the argument of the Bessel function vanish since the cyclotron radius $a \to 0$. In this limit, denoting the SP as $S_\infty(v_i)$ and assuming a spherically symmetric interaction potential, we arrive at

$$S_\infty(\mathbf{v}_i) = \frac{2\pi Z^2 \not{e}^4 n_e}{m}\ \mathcal{U} v_i \sin^2\vartheta \int \frac{1}{v^5}\left(v_{i\|} v_{e\|} - 2v_{e\|}^2 + v_i^2\right) f_e(\mathbf{v}_e) d\mathbf{v}_e. \tag{19}$$

The corresponding high-velocity asymptotic expression is given by

$$S_\infty(\mathbf{v}_i) = \frac{2\pi Z^2 \not{e}^4 n_e}{m v_i^2}\ \mathcal{U} \sin^2\vartheta. \tag{20}$$

Eqs. (15) and (19) and their asymptotic expressions for high velocities in Eqs. (18) and (20), respectively, agree with the results derived by Derbenev and Skrinsky in Ref. [57] in case of the Coulomb interaction potential, i.e., with $\mathcal{U} = \mathcal{U}_C$. Using instead a regularized interaction potential and thus the Coulomb logarithm, $\mathcal{U}_R$ allows closed analytic expressions and converging integrals and avoids any introduction of lower and upper cutoffs "by hand" in order to restrict the domains of integration. Moreover, employing the bare Coulomb interaction may, as pointed out by Parkhomchuk [58], result in asymptotic expressions which essentially different from Eqs. (19) and (20), which is related to the divergent nature of the bare Coulomb interaction (see Ref. [47]).

3.2. Some limiting cases of Eq. (11)

Next, we discuss some asymptotic regimes of the SP (Eq. (11)) where the regularized interaction (Eq. (10)) and the isotropic velocity distribution (Eq. (8)) have been assumed. In the high-velocity limit where $v_i > (\omega_c \lambda, v_{\text{th}})$, only small t contributes to the SP (Eq. (11)) due to the short time response of the electrons to the moving fast ion. In this limit we have $\sin(\alpha t)/\alpha t \to 1$. The remaining t integration can be performed explicitly. This integral is given by [47].

$$\int_0^\infty \frac{dt}{t} \Phi[\Psi(t,\zeta)] \equiv \Lambda(\varkappa). \tag{21}$$

Here, the function $\Phi(z)$ is determined by Eq. (14), and $\Lambda(\varkappa)$ is the generalized Coulomb logarithm (Eq. (17)). The remaining expressions do not depend on the magnetic field, i.e., ω_c, as a natural consequence of the short time response of the magnetized electrons. In fact,

$\sin(\alpha t)/\alpha t \to 1$ and $G(t,\zeta) \to 1$ and the related t integration (Eq. (21)) are also valid for vanishing magnetic field $\alpha \to 0$. Integration by parts turns Eq. (11) into

$$S_0 = \frac{4\pi Z^2 \not{e}^4 n_e}{m v_i^2} \Lambda(\varkappa) \left[\mathrm{erf}(v) - \frac{2}{\sqrt{\pi}} v e^{-v^2} \right], \tag{22}$$

where $\mathrm{erf}(z)$ is the error function and $v = v_i/\sqrt{2}v_{\mathrm{th}}$ is again the scaled ion velocity. The SP (Eq. (22)) is isotropic with respect to the ion velocity $\mathbf{v}_i$ and represents the two limiting cases of high velocities at arbitrary magnetic field and arbitrary velocities at vanishing field. Of course, expression (22) can be also obtained by performing the remaining integration in the nonmagnetized SP (Eq. (15)) using the isotropic velocity distribution (Eq. (8)) and $\mathcal{U} = \Lambda(\varkappa)$.

A further increase of the ion velocity finally yields

$$S_0 \simeq \frac{4\pi Z^2 \not{e}^4 n_e}{m v_i^2} \Lambda(\varkappa), \tag{23}$$

which completely agrees with the asymptotic expression (18) in case of $\mathcal{U} = \Lambda(\varkappa)$. Inspecting Eq. (23) shows that the SP does not depend explicitly on the electron temperature T at sufficiently high velocities, while T may still be involved in the generalized Coulomb logarithm $\Lambda(\varkappa)$.

At $B \to 0$ and small velocities $(v_i < v_{th})$, the SP (Eq. (22)) becomes

$$S_0 \simeq \frac{4\pi\sqrt{2\pi} Z^2 \not{e}^4 n_e}{3 m v_{\mathrm{th}}^3} v_i \Lambda(\varkappa). \tag{24}$$

Now, we consider the situation when the magnetic field is very strong and the electron cyclotron radius is the smallest length scale, $\omega_c \lambda \gg (v_i, v_{\mathrm{th}})$, and the SP is only weakly sensitive to the transverse electron velocities and, hence, is affected only by their longitudinal velocity spread. In this limit $\sin(\alpha t)/\alpha t \to 0$ and $G(t,\zeta) \to 1 - \zeta^2$ are obtained from Eq. (11) after straightforward calculations:

$$S_\infty = \frac{4\pi\sqrt{\pi} Z^2 \not{e}^4 n_e}{m v_{\mathrm{th}}^2} v \Lambda(\varkappa) \int_0^1 e^{-v^2\zeta^2 P(\zeta)} \zeta^2 d\zeta \left[2\cos^2\vartheta + P(\zeta)\left(1 - 2v^2\zeta^2\cos^2\vartheta\right) \right], \tag{25}$$

where $P(\zeta) = \cos^2\vartheta + \sin^2\vartheta/\left(1-\zeta^2\right)$.

After changing the variable ζ in Eq. (25) to $x = \zeta[P(\zeta)]^{1/2}$ and some subsequent rearrangement, Eq. (25) can be expressed alternatively as

$$S_\infty = \frac{2\sqrt{\pi} Z^2 \not{e}^4 n_e}{m v_{\mathrm{th}}^2} v \Lambda(\varkappa) \sin^2\vartheta \int_{-\infty}^{\infty} \frac{e^{-v^2x^2} x^2 dx}{1 + x^2 - 2x\cos\vartheta)^{3/2}}. \tag{26}$$

Up to the definition of the Coulomb logarithm (i.e., $\mathcal{U} = \Lambda(\varkappa)$ versus $\mathcal{U} = \mathcal{U}_C$), the expressions are identical to those obtained by Pestrikov [59].

In particular, at $\vartheta = 0$ and $\vartheta = \pi/2$ (i.e., when ion moves parallel or transverse to the magnetic field, respectively), Eq. (25) (or Eq. (26)) yields

$$S_\infty = \frac{4\sqrt{\pi}Z^2\phi^4 n_e}{mv_{\text{th}}^2}\Lambda(\varkappa)ve^{-v^2}, \tag{27}$$

$$S_\infty = \frac{2\sqrt{\pi}Z^2\phi^4 n_e}{mv_{\text{th}}^2}\Lambda(\varkappa)ve^{-v^2/2}\left[\left(1+v^2\right)K_0\left(\frac{v^2}{2}\right) - v^2K_1\left(\frac{v^2}{2}\right)\right]. \tag{28}$$

respectively, where $K_n(z)$ (with $n = 0, 1$) is the modified Bessel function. It is also constructive to obtain the angular averaged stopping power. From Eq. (25) one finds

$$\overline{S}_\infty(v) = \frac{1}{2}\int_0^\pi S_\infty(v,\vartheta)\sin\vartheta d\vartheta = \frac{4\pi Z^2\phi^4 n_e}{3mv_i^2}\Lambda(\varkappa)\left\{\text{erf}(v) + \frac{2}{\sqrt{\pi}}v\left[v^2E_1\left(v^2\right) - e^{-v^2}\right]\right\}, \tag{29}$$

where $E_1(z)$ is the exponential integral function.

In the high-velocity limit with $\omega_c\lambda \gg v_i \gg v_th$, the SP (Eq. (25)) becomes

$$S_\infty \simeq \frac{2\pi Z^2\phi^4 n_e}{mv_i^2}\Lambda(\varkappa)\left\{\sin^2\vartheta\left[\text{erf}(v) - \frac{2}{\sqrt{\pi}}ve^{-v^2}\right] + \frac{4}{\sqrt{\pi}}v^3e^{-v^2}\cos^2\vartheta\right\}. \tag{30}$$

With further increase of the ion velocity, we can then neglect the exponential term in Eq. (30), while $\text{erf}(v) \to 1$ yields the asymptotic expression (Eq. (20)) (for $\mathcal{U} = \Lambda(\varkappa)$).

The SP given by Eq. (30) (or Eq. (20) with $\mathcal{U} = \Lambda(\varkappa)$) decays as the corresponding SP (Eq. (23)) like $\sim v_i^{-2}$ with the ion velocity. But here, the parallel SP (Eq. (27)) vanishes exponentially at $\vartheta = 0$ which is a consequence of the presence of a strong magnetic field, where the electrons move parallel to the magnetic field. If the ion moves also parallel to the field (i.e., $\vartheta = 0$), the averaged stopping force must vanish within the BC treatment for symmetry reasons.

Finally, we also investigate the case of small velocities at strong magnetic fields. Considering a small ion velocity ($v \ll 1$) in Eq. (25), we arrive at

$$S_\infty = \frac{4\pi Z^2\phi^4 n_e}{mv_{\text{th}}^2}\Lambda(\varkappa)v\left\{\sin^2\vartheta\left[ln\left(\frac{2}{v\sin\vartheta}\right) - \frac{\gamma}{2} - 1\right] + \cos^2\vartheta\right\}, \tag{31}$$

where $\gamma \simeq 0.5772$ is Euler's constant. Now, it is seen that the SP, S^∞, leads at low ion velocities $v \ll 1$ and for a nonzero ϑ to a term which behaves as $\sim v\ln(1/v)$. Thus, the corresponding friction coefficient diverges logarithmically at small v. This is a quite unexpected behavior compared to the well-known linear velocity dependence without magnetic field (see asymptotic expressions above). Finally, at $\vartheta = 0$ the logarithmic term vanishes and the SP behaves as $S^\infty \sim v$.

4. Features of the SP (Eq. (11)) and comparison with CTMC simulations

In this section we study some general properties of the SP of individual ions resulting from the BC approach by evaluating Eq. (11) numerically. We consider the effect of the magnetic field on the SP at various temperatures of the plasma. The density $n_e \simeq 10^{16}\text{cm}^{-3}$ and the temperatures $T \simeq 1\,\text{eV}$, 10 or 100 eV of the electron plasma, are in the expected range of the envisaged experiments on proton or alpha particles stopping in a magnetized target plasma [46] (see corresponding **Figures 1–3**). As an example we choose proton projectile for our calculations. In all examples considered below, the regularization parameter $\lambda\!\!\!^{-}_0 = 10^{-10}\,\text{mm}$ thereby meets the condition $\lambda\!\!\!^{-}_0 \gg b_0(0)$, i.e., $\lambda\!\!\!^{-}_0$, and does not affect noticeably the SP (Eq. (11)) at low and medium velocities as shown in Appendix A (see also Ref. [47] for more details).

For a BC description beyond the perturbative regime, a fully numerical treatment is required. In the present cases of interest, such a numerical evaluation of the SP is rather intricate but can be successfully implemented by classical trajectory Monte Carlo (CTMC) simulations [37–40]. In the CTMC method, the trajectories for the ion-electron relative motion are calculated by a numerical integration of the equations of motion (Eq. (2)). The stopping force is then deduced by averaging over a large number (typically 10^5–10^6) of trajectories employing a Monte Carlo

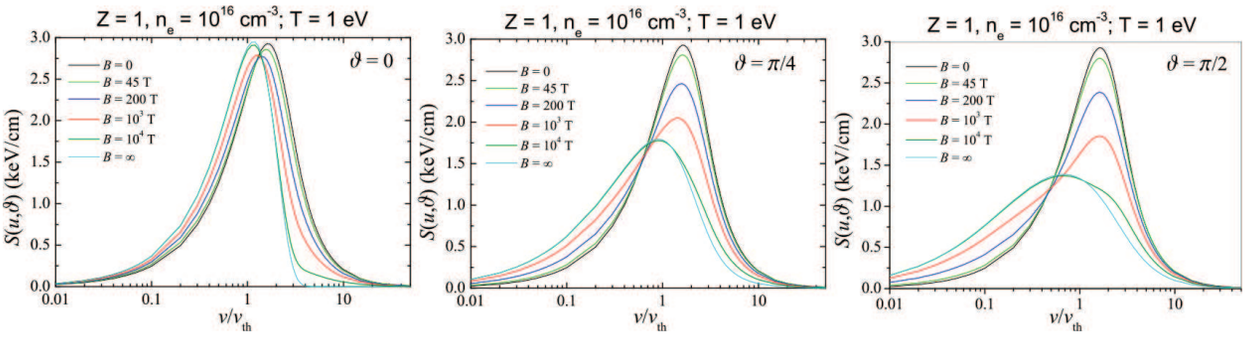

Figure 1. The SP [in keV/cm] for protons as a function of the ion velocity v_i [in units of v_{th}] and for fixed plasma temperature $T = 1\,\text{eV}$. The theoretical stopping power (Eq. (11)) is calculated for $\lambda\!\!\!^{-}_0 = 10^{-10}\text{m}$ (see appendix a for details) and for an electron plasma with $n_e = 10^{16}cm^{-3}$ in a magnetic field of $B = 0$ (black), 45 T (green), 200 T (blue), 10^3 T (red), 10^4 T (green), and $B = \infty$ (cyan). The angle ϑ between **B** and $\mathbf{v_i}$ is $\vartheta = 0$ (left), $\vartheta = \pi/4$ (center), and $\vartheta = \pi/2$ (right). The CTMC results for $B = \infty$ case are shown by the filled circles.

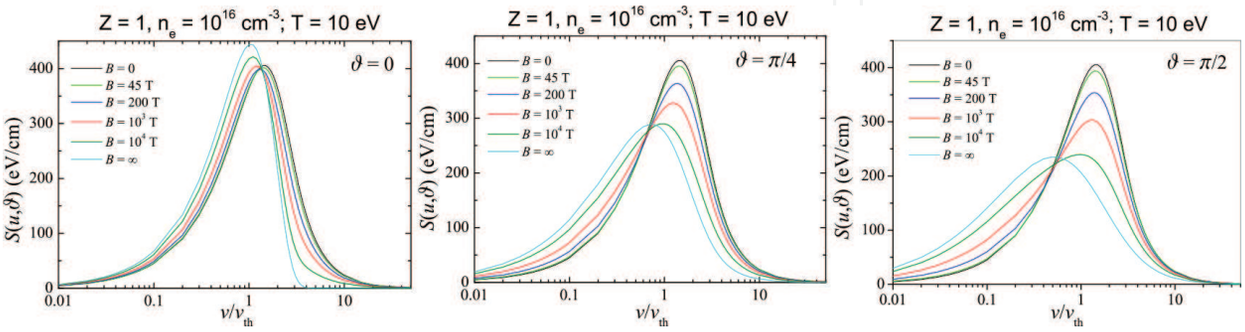

Figure 2. Same as in **Figure 1** but for $T = 10\,\text{eV}$. The SP is given in units eV/cm.

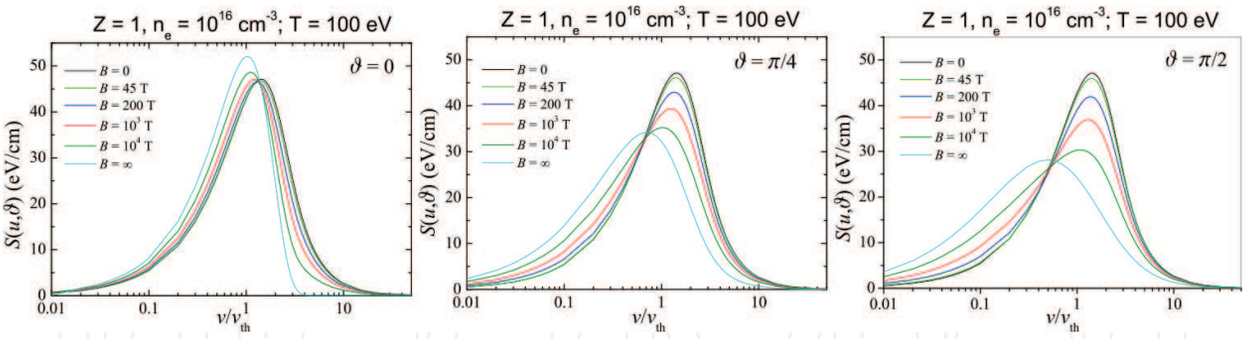

Figure 3. Same as in **Figure 1** but for $T = 100$ eV. The SP is given in units eV/cm.

sampling for the related initial conditions. For a more detailed description of the method, we refer to Refs. [8, 44, 45]. Both the analytic perturbative treatment and the non-perturbative numerical CTMC simulations are based on the same BC picture and use the same effective spherical screened interaction $U(r)$. The following comparison of these both approaches thus essentially intends to check the validity and range of applicability of the perturbative approach as it has been outlined in the preceding sections.

5. Stopping profiles and ranges

5.1. General trends

The parameter analysis initiated on **Figures 1–3** at $n_e = 10^{16} cm^{-3}$ and $T = 1 - 10 - 100$ eV is implemented for monitoring a possible experimental vindication through a fully ionized hydrogen plasma out of high-power laser beams available on facilities such as ELFIE (Ecole Polytechnique) or TITAN (Lawrence Livermore) [62]. The given adequately magnetized targets (in the 20–45 T range) would then be exposed to TNSA laser-produced proton beams out of the same facilities, in the hundred keV-MeV energy range [62].

Therefore, we are looking for the most conspicuous effect of the applied magnetized intensity B on the proton stopping.

Fixing n_e and varying T (see **Figures 1–3**) display an ubiquitous and increasing anisotropy shared by the stopping profiles (SP) with increasing B and θ and angle between $\vec{B}$ and initial projectile velocity $\vec{V}$.

Moreover, that anisotropy evolves only moderately between $\theta = \frac{\pi}{4}$ and $\frac{\pi}{2}$.

Another significant feature is the extension to any $B \neq 0$ of the $B = 0$ scaling $\frac{n_e}{T}$. For instance, SP at $n_e = 10^{12}$ cm^{-3} and T = 1 eV, at a given θ, is equivalent to that for $n_e = 10^{14}$ cm^{-3} and T = 100 eV.

As expected, B effects impact essentially the low-velocity section ($\frac{V}{V_{th}}$, V_{th} = target electron thermal velocity) of the ion stopping profile. One can observe, increasing with B, a shift to the

left of SP maxima, as shown in **Figure 4** at B = 45 tesla, for the profiles displayed in **Figure 3**, with θ-averaged SP remaining close to $\theta = \frac{\pi}{2}$.

Switching now attention to corresponding ranges, down to projectile at rest $(E_p = 0)$, one witnesses on **Figure 5** the counterpart of the above-noticed SP behavior.

In a low projectile velocity $\left(\frac{V}{V_{th}} \leq 1\right)$, one gets the largest B effects and the smallest proton ranges attributed to the highest B. The fan of B ranges then merges on a given point, located between 10 keV and 100 keV at $n_e = 10^{16} cm^{-3}$, and then inverts itself with increasing B featuring now increasing ranges. Moreover, the aperture of the fan of ranges increases steadily with θ.

Finally, it can be observed that for $\theta = 0$, the infinite magnetized range looks rather peculiar and reminiscent of the ion projectile gliding on $\vec{B} \parallel \vec{V}$ [8, 34].

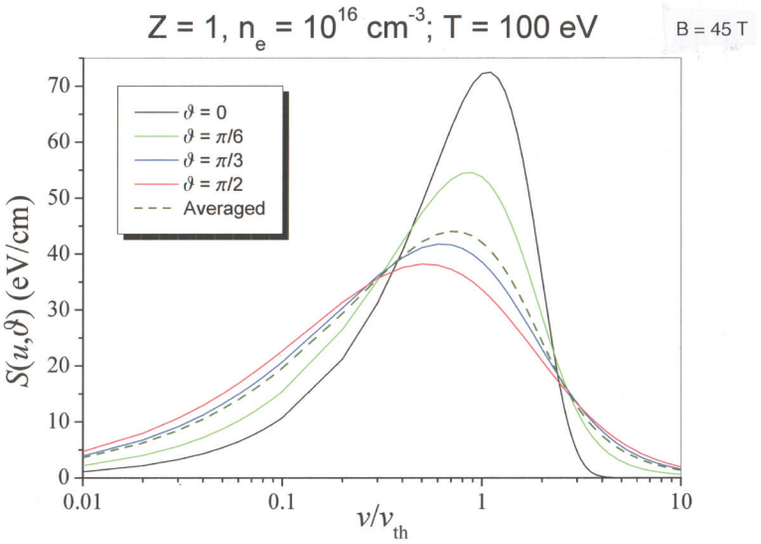

Figure 4. Same as in **Figure 3** restricted to B = 45 T, featuring θ-dependent and θ-averaged SP in eV/cm.

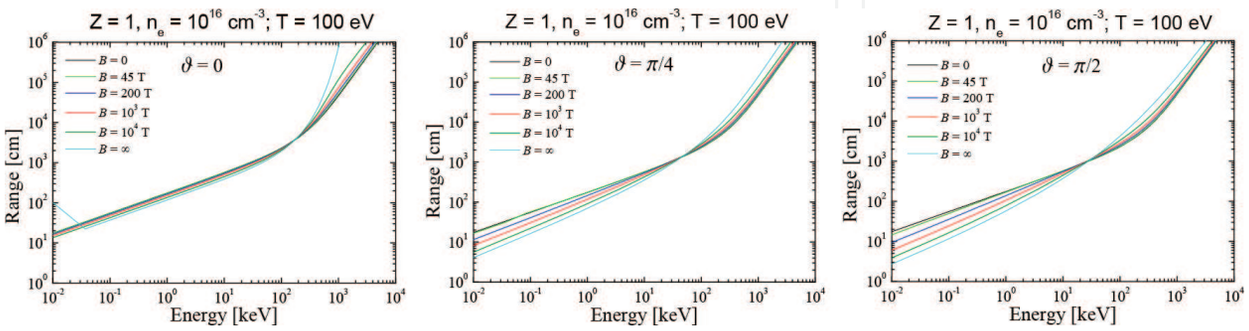

Figure 5. Ranges, down to zero energy pertaining to SP in **Figure 3**.

http://dx.doi.org/10.5772/intechopen.77213

5.2. Specific trends

The projected experimental setup [62] could manage constant, static, and homogeneous B values up to 45 T. So, we are let to investigate n_e range limits within which significant B effects can be observed.

Obviously, $n_e = 10^{12}$ cm^{-3} is expected to show quantitatively larger B impact than 10^{18} cm^{-3}.

Giving attention to proton ranges of T dependence in a low-density plasma $\left(n_e = 10^{12}\text{cm}^{-3}\right)$ at T = 1 and 100 eV, respectively, (**Figure 6**), one witnesses the smallest ranges for $\frac{V}{V_{th}} \ll 1$, increased by four orders of magnitude between 1 and 100 eV while remaining essentially unchanged for $\frac{V}{V_{th}} \geq 1$. Turning now to $n_e = 10^{18}\text{cm}^{-3}$ at T = 1 eV, one can see that the given SP remains quasi-isotropic, hardly θ-dependent, except at extreme magnetization (B = ∞). Discrepancies between B = 0 and 20 T remain visible only for $\frac{V}{V_{th}} \leq 2$. B = ∞ does not feature anymore the highest stopping when $\frac{V}{V_{th}} \leq 1$. Also, $B = 10^3$ SP exhibits a few top wigglings. Upshifting T at 10 eV yields back $n_e = 10^{18}\text{cm}^{-3}$ SPs very similar to these displayed on **Figure 2** ($n_e = 10^{16}$ cm^{-3}, T = 10 eV) **Figure 7**.

Corresponding proton ranges ($n_e = 10^{18}$ cm^{-3}, T = 1 eV) are shown in **Figure 8**.

Experimentally, accessible and very small ranges are thus documented for $\frac{V}{V_{th}} \leq 1$. Here, B = 0 and 20 T data remain everywhere distinguishable.

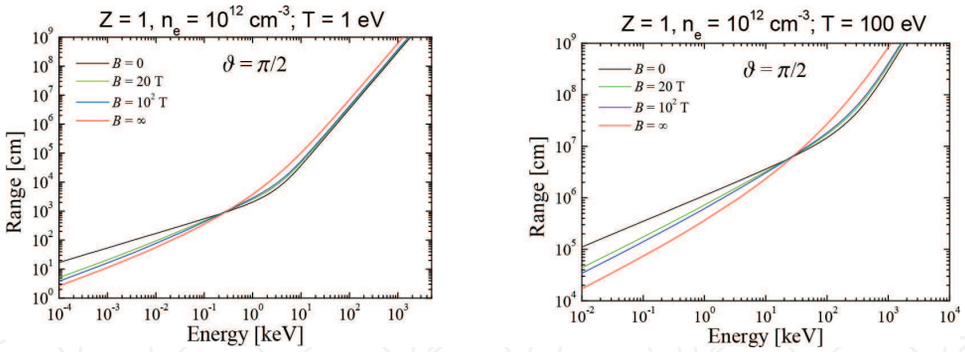

Figure 6. Proton ranges down to the rest of the target with $n_e = 10^{12}$ cm^{-3}, T = 1, and 100 eV at $\theta = \frac{\pi}{2}$.

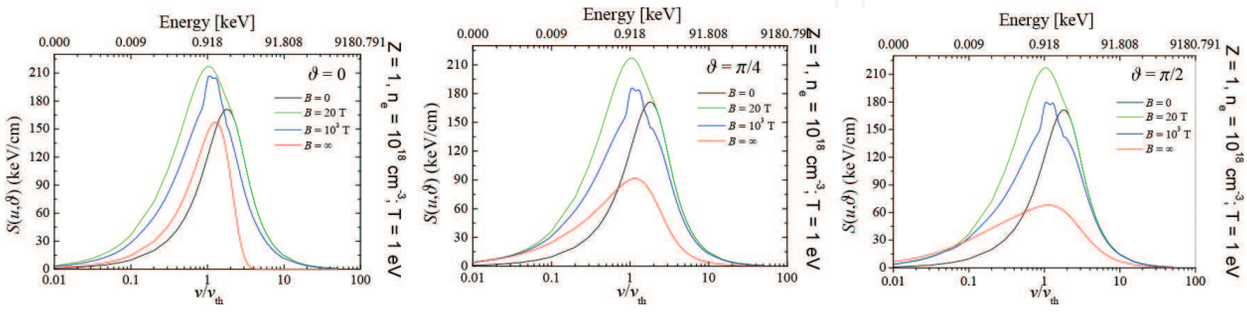

Figure 7. Same as in **Figure 1** for $n_e = 10^{18}$ cm^{-3} and T = 1 eV with $\theta = 0, \frac{\pi}{4}$, and $\frac{\pi}{2}$.

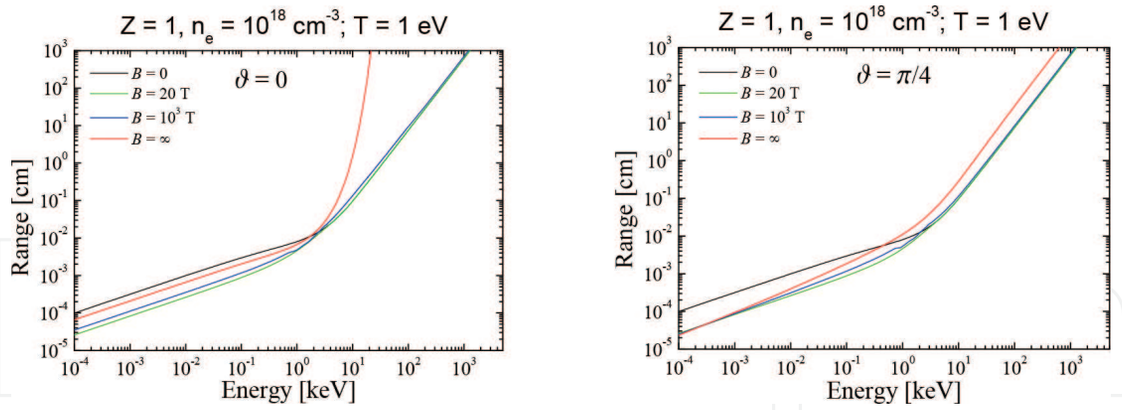

Figure 8. Proton ranges in electron target $n_e = 10^{12}$ cm^{-3} and T = 1 eV with $\theta = 0$ and $\frac{\pi}{4}$.

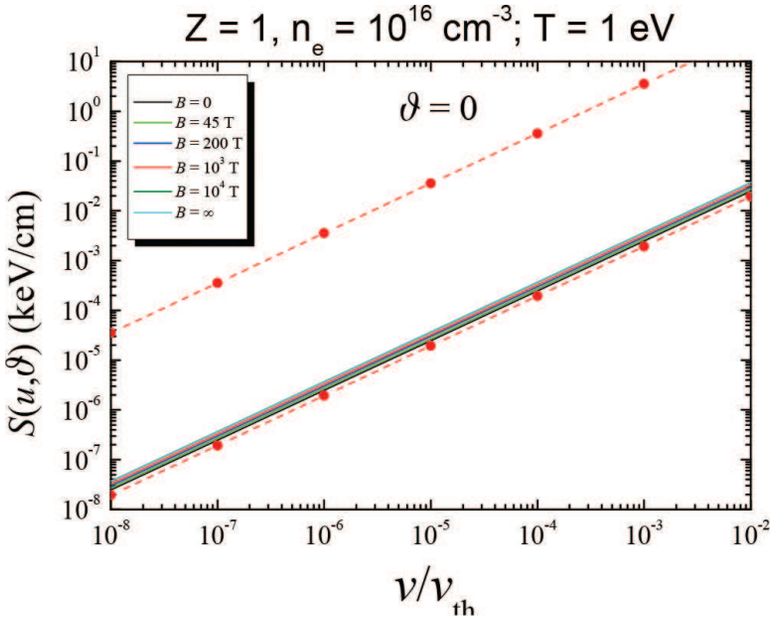

Figure 9. Very-low-velocity proton slowing down on target protons at B = 10^3T (upper straight line) contrasted to target electron stopping (any B, lower straight lines).

5.3. Very-low-velocity proton slowing down

Up to now we limited our investigation to proton stopping by target electrons. In the very-low-velocity regime $V \leq V_{thi}$, the target protons can also contribute significantly as evidenced on **Figure 9**. This topic will be more thoroughly addressed in a separate presentation.

6. Summary

We developed and extensively used a kinetic approach based on a binary collision formulation and suitably regularized Coulomb interaction, to numerically document for any value of the

applied magnetization B, the stopping of a proton projectile in a fully ionized hydrogen plasma target. Both ion projectile and target plasma parameters have been selected in order to fit a planned ion-plasma interaction experiment in the presence of an applied magnetic field $\tilde{B}$. It should be pointed out that we restricted the target plasma to its electron component. It therefore remains to include the target ion contribution to proton stopping [63], thus featuring a complete low-velocity ion slowing down.

More generally, we expect that the present investigation, experimentally geared as it is, could help to bridge a long-standing and persisting gap between theoretical speculations and experimental facts in the field of nonrelativistic ion stopping in magnetized target plasmas.

Acknowledgements

The work of H.B.N. has been supported by the State Committee of Science of the Armenian Ministry of Education and Science (Project No. 13-1C200). This work was supported by the Bundesministerium für Bildung und Forschung (BMBF) under contract 06ER9064.

Appendix A: Adjustment of the effective interaction

Our results (Eq. (11)) were derived by using the screened interaction $U_{\mathrm{R}}(r)$. As already mentioned, the use and the modeling of such an effective two-body interaction are a major but indispensable approximation for a BC treatment where the full ion-target interaction is replaced by an accumulation of isolated ion-electron collisions. The replacement of the complicated real non-spherically symmetric potential, like the wake fields as shown and discussed in Ref. [60], with a spherically symmetric one is, however, well motivated by earlier studies on a BC treatment at vanishing magnetic field (see Refs. [53–55]). It was shown by comparison with 3D self-consistent PIC simulations that the drag force from the real nonsymmetric potential induced by the moving ion can be well approximated by an BC treatment employing a symmetric Debye-like potential with an effective velocity-dependent screening length $\lambda(v_i)$. In these studies also a recipe was given how to derive the explicit form of $\lambda(v_i)$, which turned out to be not too much different from a dynamic screening length of the simple form $\lambda(v_i) = \lambda_{\mathrm{D}}\left[1 + (v_i/v_{th})^2\right]^{1/2}$. Here, $\lambda_{\mathrm{D}} = v_{\mathrm{th}}/\omega_p$ is the Debye screening length at $v_i = 0$, ω_p is the electron plasma frequency, and v_{th} is a thermal velocity of electrons. Although no systematic studies about the use of such an effective interaction with a screening length $\lambda(v_i)$ have been made for ion stopping in a magnetized electron plasma, the replacement of the real interaction by a velocity-dependent spherical one should be a reasonable approximation also in this case. The introduced dynamical screening length $\lambda(v_i)$ also implies the assumption of a weak perturbation of the electrons by the ion and linear screening where the screening length is independent of the ion charge Ze, which coincide with the regimes of perturbative BC (see, e.g., Ref. [54]). Therefore, we do not consider here possible nonlinear screening effects.

Next, we specify the parameter λ which is a measure of the softening of the interaction potential at short distances. As we discussed in the preceding sections, the regularization of the potential (Eq. (10)) guarantees the existence of the s integrations, but there remains the problem of treating accurately hard collisions. For a perturbative treatment, the change in relative velocity of the particles must be small compared to v_r, and this condition is increasingly difficult to fulfill in the regime $v_r \to 0$. This suggests to enhance the softening of the potential near the origin of the smaller v_r. Within the present perturbative treatment, we employ a dynamical regularization parameter $\lambda(v_i)$ [44, 45], where $\lambda^2(v_i) = Cb_0^2(v_i) + \lambda_0^2$ and $b_0(v_i) = |Z|\phi^2/m(v_i^2 + v_{\text{th}}^2)$. Here, b_0 is the averaged distance of the closest approach of two charged particles in the absence of a magnetic field, and λ_0 is some free parameter. In addition we also introduced $C \simeq 0.292$ in $\lambda(v_i)$. In Refs. [44, 45], this parameter is deduced from the comparison of the second-order scattering cross sections with an exact asymptotic expression derived in Ref. [61] for the Yukawa type (i.e., with $\lambda \to 0$) interaction potential. As we have shown in Refs. [44, 45] employing the dynamical parameter (v_i), the second-order cross sections for electron-electron and electron-ion collisions excellently agree with CTMC simulations at high velocities. Also, the free parameter λ_0 is chosen such that $\lambda_0 \ll b_0(0)$, where $b_0(0)$ is the distance $b_0(v_i)$ at $v_i = 0$. From the definition of (v_i), it can be directly inferred that λ_0 does not play any role at low velocities, while it somewhat affects the size of the stopping force at high velocities when $b_0(v_i) \lesssim \lambda_0$. More details on the parameter λ_0 and its influence on the cooling force are discussed in Ref. [47].

Author details

Hrachya B. Nersisyan[1,2]*, Günter Zwicknagel[3] and Claude Deutsch[4]

*Address all correspondence to: hrachya@irphe.am

1 Plasma Theory Group, Institute of Radiophysics and Electronics, Ashtarak, Armenia

2 Centre of Strong Fields Physics, Yerevan State University, Yerevan, Armenia

3 Institut für Theoretische Physik II, Universität Erlangen-Nürnberg, Erlangen, Germany

4 LPGP, Université Paris-Saclay, Orsay, France

References

[1] Killian TC. Ultracold neutral plasmas. Science. 2007;**316**:705

[2] Deutsch C, Nersisyan HB, Zwicknagel G. Equilibrium and transport in strongly coupled and magnetized ultracold plasmas. In: Shukla PK, Mendonça JT, Eliasson B, Resedes D, editors. Strongly Coupled Ultra-Cold and Quantum Plasmas. Vol. 1421. AIP Conf. Proc; 2012. p. 3

[3] Sørensen AH, Bonderup E. Electron cooling. Nuclear Instruments & Methods. 1983;**215**:27

[4] Poth H. Electron cooling, Theory, Experiment, Application. Physics Reports. 1990;**196**:135

[5] Meshkov IN. Electron cooling, status and perspectives. Physics of Particles and Nuclei. 1994;**25**:631

[6] Men'shikov LI. Electron cooling. Physics-Uspekhi. 2008;**51**:645

[7] Zwicknagel G. Electron cooling of ions and antiprotons in traps. In: Nagaitsev S, Pasquinelli RJ, editors. Beam Cooling and Related Topics. Vol. 821. AIP Conf. Proc.; 2006. p. 513

[8] Nersisyan HB, Toepffer C, Zwicknagel G. Interactions between Charged Particles in a Magnetic Field: A Theoretical Approach to Ion Stopping in Magnetized Plasmas. Heidelberg: Springer; 2007

[9] Möllers B, Walter M, Zwicknagel G, Carli C, Toepffer C. Drag force on ions in magnetized electron plasmas. Nuclear Instruments and Methods in Physics Research Section B: Beam Interactions with Materials and Atoms. 2003;**207**:462

[10] Mollers B, Toepffer C, Walter M, Zwicknagel G, Carli C, Nersisyan HB. Cooling of ions and antiprotons with magnetized electrons. Nuclear Instruments and Methods in Physics Research Section A: Accelerators, Spectrometers, Detectors and Associated Equipment. 2004;**532**:279

[11] Cereceda C, Deutsch C, DePeretti M, Sabatier M, Nersisyan HB. Dielectric response function and stopping power of dens magnetized plasmas. Physics of Plasmas. 2000;**7**:2884

[12] Cereceda C, DePeretti M, Deutsch C. Stopping power for arbitrary angle between test particle velocity and magnetic field. Physics of Plasmas. 2005;**12**:022102

[13] Rostoker N, Rosenbluth MN. Test particle in a completely ionized plasma. Physics of Fluids. 1960;**3**:1

[14] Rostoker N. Kinetic equation with a constant magnetic field. Physics of Fluids. 1960;**3**:922

[15] Akhiezer IA, Eksp Z. Theory of the interaction of a charged particle with a plasma in a magnetic field. Teor. Fiz. 1961;**40**:954; Sov. Phys. JETP 1961;**13**:667

[16] Akhiezer AI, Akhiezer IA, Polovin RV, Sitenko AG, Stepanov KN. Plasma Electrodynamics. 1st ed. Vol. 1. Pergamon: Oxford; 1975

[17] Honda N, Aona O, Kihara T. Fluctuations in a plasma 3: Effect of a magnetic field on stopping power. Journal of the Physical Society of Japan. 1963;**18**:256

[18] May RM, Cramer NF. Test ion energy loss in a plasma with a magnetic field. Physics of Fluids. 1970;**13**:1766

[19] Boine-Frankenheim O, DAvanzo J. Stopping power of ions in a strongly magnetized plasma. Physics of Plasmas. 1996;**3**:792

[20] Nersisyan HB. Stopping of charged particles in a magnetized classical plasma. Physical Review E. 1998;**58**:3686

[21] Nersisyan HB. Stopping of heavy ions in a magnetized strongly coupled plasmas: high velocity limit. Contributions to Plasma Physics. 2005;**45**:46

[22] Nersisyan HB, Deutsch C. Correlated fast ion stopping in magntized classical plasma. Physics Letters A. 1998;**246**:325

[23] Nersisyan HB, Walter M, Zwicknagel G. Stopping power of ions in a magnetized two-temperature plasma. Physical Review E. 2000;**61**:7022

[24] Nersisyan HB, Zwicknagel G, Toepffer C. Energy loss of ions in a magntized plasma: Conformity between linear response and binary collision treatment. Physical Review E. 2003;**67**:026411

[25] Nersisyan HB. Ion stopping in a dense magnetized plasmas. Nuclear Instruments and Methods in Physics Research Section B: Beam Interactions with Materials and Atoms. 2003;**205**:276

[26] Nersisyan HB, Zwicknagel G, Toepffer C. Conformity between linear response and binary collision treatment of an ion energy loss in a magnetized quantum plasma. European Physical Journal D: Atomic, Molecular, Optical and Plasma Physics. 2004;**28**:235

[27] Nersisyan HB, Deutsch C, Das AK. Number-conserving linear response study of low velocity ion stopping in a collisional magnetized classical plasma. Physical Review E. 2011;**83**. DOI: 036403

[28] Nersisyan HB, Deutsch C. Low velocity ion stopping in a a collisional plasma. European Physical Journal: Web of Conferences. 2013;**59**:05019

[29] Nersisyan HB, Deutsch C. Energy loss of ions by electric field fluctuations in a magnetized plasma. Physical Review E. 2011;**83**:066409

[30] Seele C, Zwicknagel G, Toepffer C, Reinhard P-G. Time-dependent stopping power and influence of an infinite magnetic field. Physical Review E. 1998;**57**:3368

[31] Walter M, Toepffer C, Zwicknagel G. Stopping power of ions in a magnetized two-temperature plasmas. Nuclear Instruments and Methods in Physics Research Section B: Beam Interactions with Materials and Atoms. 2000;**168**:347

[32] Walter M. Ph.D. thesis. Ion stopping in a magnetized plasma. University of Erlangen; 2002

[33] Steinberg M, Ortner J. Energy loss of a charged particle in magnetized quantum plasma. Physical Review E. 2001;**63**:046401

[34] Deutsch C, Popoff R. Low ion-velocity slowing down in a strongly magnetized plasma target. Physical Review E. 2008;**78**:056405

[35] Deutsch C, Popoff R. Low ion-velocity slowing down in a classical plasma. Nuclear Instruments and Methods in Physics Research Section A: Accelerators, Spectrometers, Detectors and Associated Equipment. 2009;**606**:212

[36] Deutsch C, Zwicknagel G, Bret A. Ultracold plasmas: A paradigm for strongly coupled and classical electron fluids. Journal of Plasma Physics. 2009;**75**:799

[37] Zwicknagel G. Theory and Simulation of the Interaction of Ions with Plasmas: Nonlinear Stopping, Ion-Ion Correlation Effects and Collisions of Ions with Magnetized Electrons, Habilitation Treatise. University of Erlangen; 2000. [http://www.opus.ub.uni-erlangen.de/opus/volltexte/2008/913/]

[38] Zwicknagel G. Ion-electron collisions in a homogeneous magnetic field. In: Bollinger JB, Spencer RL, Davidson RC, editors. Non-Neutral Plasma Physics III. Vol. 498. AIP Conf. Proc.: 1999. p. 469

[39] Zwicknagel G. Nonlinear energy loss of highly charged heavy ions. Nuclear Instruments and Methods in Physics Research Section A: Accelerators, Spectrometers, Detectors and Associated Equipment. 2000;**441**:44

[40] Zwicknagel G, Toepffer C. Energy loss of ions by collisions with magnetized electrons. In: Anderegg F, Schweikhard L, Driscoll CF, editors. Non-Neutral Plasma Physics IV. Vol. 606. AIP Conf. Proc.; 2002. p. 499

[41] Zwicknagel G. Trapped charged particles and fundamental interactions. In: Blaum K, Herfurth F, editors. Trapped Charged Particles and Fundamental Interactions, Lecture Notes in Physics. Vol. 749. Berlin: Springer-Verlag; 2008. pp. 69-96

[42] Toepffer C. plaScattering of magnetized electrons by ions. Physical Review A. 2002;**66**: 022714

[43] Nersisyan HB, Zwicknagel G. Conformity between linear response and binary collision treatments of an ion energy loss in a magnetized quantum plasma. Journal of Physics A: Mathematical and General. 2004;**37**:11073

[44] Nersisyan HB, Zwicknagel G. Binary collisions of charged particles in a magnetic field. Physical Review E. 2009;**79**:066405

[45] Nersisyan HB, Zwicknagel G. Energy transfer in binary collisions of two gyrating charged particles in a magnetic field. Physics of Plasmas. 2010;**17**:082314

[46] Deutsch C, Nersisyan HB, Bendib A. Diagnostics of arbitrary magnetized and dense plasmas of ICF/WDM concern. In: Proceedings of the 20th International Symposium on Heavy- Ion Inertial Fusion, HIF 2014, Lanzhou, China, 11–15 August, 2014. DOI: http://dx.doi.org/10.1017/S0263034615000919 in Laser Part. Beams 2015

[47] Nersisyan HB, Zwicknagel G. Cooling force on ions in a magnetized electron plasma. Physical Review Accelerators and Beams. 2013;**16**:074201

[48] Winkler T. Ph.D. thesis; Electron cooling of highly charged ions. University Heidelberg; 1996

[49] Winkler T et al. Electron cooling force measurements for highly charged ions in the ESR. Hyperfine Interactions. 1996;**99**:277

[50] Winkler T, Beckert K, Bosch F, Eickhoff H, Franzke B, Nolden F, Reich H, Schlitt B, Steck M. Electron cooling of highly chargd ions in the ESR. Nuclear Instruments and Methods in Physics Research Section A: Accelerators, Spectrometers, Detectors and Associated Equipment. 1997;**391**:12

[51] Kelbg G. Theorie des quanten plasmas. Annalen der Physik (Berlin). 1963;**467**:219

[52] Deutsch C. Nodal expansion in a real matter plasma. Physics Letters A. 1977;**60**:317

[53] Zwicknagel G. Theory and simulation of heavy ion stopping in plasma. Laser and Particle Beams. 2009;**27**:399

[54] Zwicknagel G. Nonlinear energy loss of heavy ions in plasmas. Nuclear Instruments and Methods in Physics Research Section B: Beam Interactions with Materials and Atoms. 2002;**197**:22

[55] Zwicknagel G, Toepffer C, Reinhard P-G. Stopping of heavy ions in plasmas at strong coupling. Physics Reports. 1999;**309**:117; 1999;**314**:671(E)

[56] Gradshteyn IS, Ryzhik IM. Tables of Integrals, Series and Products. 2nd ed. New York: Academic; 1980

[57] Derbenev YS, Skrinsky AN. The effect of a magnetic field on electron cooling. Particle Accelerator. 1978;**8**:235

[58] Parkhomchuk VV. In: Poth H, editor. Proceedings of the Workshop on Electron Cooling and Related Applications (ECOOL84, 1984). Karlsruhe: KfK; 1985. p. 71; KfK Report No. 3846

[59] Pestrikov DV. Longitudinal cooling force due to magnetized electrons. Nuclear Instruments and Methods in Physics Research Section A: Accelerators, Spectrometers, Detectors and Associated Equipment. 2005;**554**:13

[60] Peter T, Meyer-ter-Vehn J. Energy loss of heavy ions in dense plasmas 1. Linear and nonlinear Vlasov theory for the stopping power. Physical Review A. 1991;**43**:1998

[61] Hahn H, Mason EA, Smith FJ. Quantum transport cross sections for ionized gases. Physics of Fluids. 1971;**14**:278

[62] Chen S, Fuchs J. Ecole Polytechnique. Private Communication; July 2014

[63] Tashev B, Baimbetov F, Deutsch C, Fromy P. Low velocity ion stopping in binary ionic mixtures. Physics of Plasmas. 2008;**15**:102701